Very-Near-Field Plume Model of a Hall Thruster

F. Taccogna[1], S. Longo[1,2], M. Capitelli[1,2]
[1] Department of Chemistry, University of Bari, Italy
[2] IMIP-CNR sect. Bari, Italy

Plasmadynamic phenomena of a stationary plasma thruster (SPT-100) plume in the very-near-field region have been studied by using a two-dimensional axysimmetric numerical code based on a combination of Particle in Cell (PIC) simulation for ion component (Xe^+ and Xe^{++}) and fluid description for electrons. The model can reproduce qualitatively several experimental observations.

1. Introduction

Stationary plasma thrusters (also called closed electron drift thruster of the Morozov type) [1] are ion thrusters with high specific impulse and low thrust that make them suitable for satellite station keeping or orbit transfer.

A major concern in the use of these devices is the possible damage their plumes may cause to the host spacecraft and to communication interference of satellites. Indeed an electric thruster, such SPT-100, in operation produces, besides high energy ions (Xenon for his inert and low ionization potential property) responsible of the thrust and electrons emitted to neutralize the positive space charge, also neutral propellant atoms and low energy ions created by charge exchange (CEX) collisions between ions and un-ionized propellant (in which electrons are transferred) or by electron impact ionization of neutral atoms. They are more influenced by the self-consistent electric fields that cause slow ions to propagate radially and to flow upstream, while gaining energy.

Thus, the structure of the plasma plume exhaust from the thruster is of great interest and several models [2-5] have been developed simulating the plasmadynamic of the exhaust plume in the far-field region. The modelling of the plasma plume of electric thrusters in the very-near-field plume region (z<0.2 m from the thruster exit plane) is important because there are many new aspects to take in account as plasma sheath effect, magnetic field effect, non isothermal electrons, electron-neutral collisions and so on.

2. Numerical model

Due to particular geometry of the problem each quantity is given in terms of axisymmetric coordinates (r,z) and we assume no variation in the azimuthal direction.

In the PIC technique, ions are considered as macro-particle and their charge are deposited onto a computational grid using the cylindrical weighting functions. Ions are loaded into the simulation at each time step to simulate the exit flow. The ion exit conditions (radial position and velocity components) are given in ref. [5] on the basis of fitted experimental data.

In order to know the electron charge density, one differentiates the momentum conservation equation and substituting the laplacian of the electric potential with the source term of Poisson equation the following differential non linear equation for the electron charge density results:

$$\frac{k_B T_e}{e}\nabla^2 ln\rho_e + \frac{k_B}{e}\nabla ln\rho_e \cdot \nabla T_e - \frac{\rho_e}{\varepsilon_0} - B_r\frac{\partial v_{ei}}{\partial z} + \frac{k_B}{e}\nabla^2 T_e + \frac{\rho_i}{\varepsilon_0} = 0 \quad (1)$$

with boundary conditions given by (see Fig. 1):

$$\begin{cases} S_1 \rightarrow \rho_e = -\rho_i \\ S_2 \rightarrow \rho_e = \rho_\infty \\ L_1 \rightarrow \dfrac{\partial \rho_e}{\partial r} = 0 \\ L_2, L_3, L_4 \rightarrow \rho_e = \rho_\infty \end{cases}$$

In eq. (1), $v_{e,t}=v_{i,t}$ since the particle flow across the magnetic field is ambipolar (current-less) and we consider only the radial component of the magnetic field (dipol approximation).

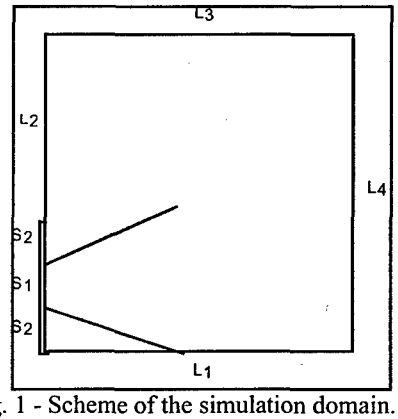

Fig. 1 - Scheme of the simulation domain.

The solution is obtained by the iterative Newton-Raphson method discretizing the laplacian with a 5-points formula in cylindrical coordinates and using a successive-over-relaxation (SOR) scheme.

Once the electron charge density is computed, the electrostatic potential is determined by solving Poisson's equation.

Knowing the electron density we can solve the electron energy conservation equation for the temperature where we neglect the unsteady and convection terms and we consider the following ionization energy sink term:

$$Q_e = \dot{n}_e E_i \quad (2)$$

with $\dot{n}_e = k_{T_e} n_e n_{Xe}$ the volumetric ionization rate and E_i the Xenon ionization energy. We calculate the electron impact ionization rate coefficient $k(T_e)$ on the basis of e/Xe cross-section data [6] fitted to the following polynomial expression:

$$k(T_e) = 4.5243\times10^{-15} - 4.4952\times10^{-15}T_e + 1.1776\times10^{-15}T_e^2 - 2.5515\times10^{-17}T_e^3 - 2.3932\times10^{-18}T_e^4 + 9.7869\times10^{-20}T_e^5 \quad (3)$$

Substituting the ideal gas equation we have

$$\kappa_e \nabla^2 T_e + \nabla\kappa_e \cdot \nabla T_e = -Q_e \quad (4)$$

where the electron thermal conductivity is included by the following fitting formula (including the electron collision effect) [7]:

$$\kappa_e = AT_e^n \quad \text{with} \quad \begin{cases} A = 6.9\times10^{-12} & n = 5/2, \quad T_e \le 2eV \\ A = 2.08\times10^{-3} & n = 1/2, \quad T_e > 2eV \end{cases} \quad (5)$$

Eq. (4) is solved with the following boundary conditions:

$$\begin{cases} S_1, S_2 \rightarrow T_e = const \\ L_1 \rightarrow \dfrac{\partial T_e}{\partial r} = 0 \\ L_2, L_3, L_4 \rightarrow T_e = T_\infty \end{cases}$$

and we come back to the electron momentum conservation equation until we reach convergency.

The ions are moved under the influence of the self-consistent electric field integrating numerically the equations of motion using the leap-frog algorithm .

Collisional processes are modeled between move steps using a TPMC method [8] to simulate Xe-Xe^+ and Xe-Xe^{++} (momentum and charge transfer) collisions, and a volumetric production method to simulate neutral ionization by electron impact.

3. Results

The behavior of the plasma potential is reported in Fig. 2. We can see the potential wall structure developing spontaneously that capture ions to neutralize electrons trapped by magnetic field. In fact we note a peak near the centerline at the small axial position that is attributed to electrons confined by magnetic field cusp formed by the thruster magnetic coils.

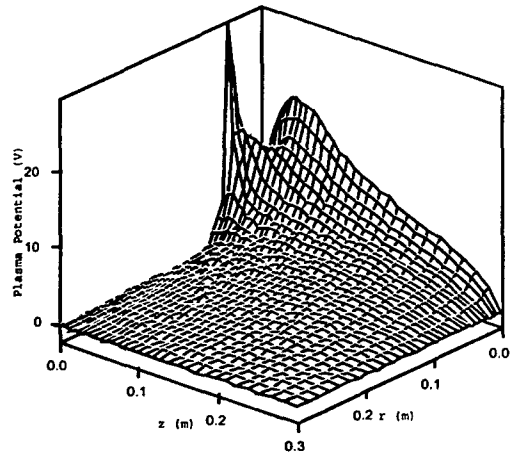

Fig. 2 - Plasma potential surface.

Figure 3 shows the radial profiles of electron temperature measured [9] at different axial locations The peak structure in front of the discharge channel (28mm<r<50mm) decreases in magnitude and broadens as the electrons move away axially from the thruster in agreement to the fact that electrons continue to cool down. We note a discrepancy between the model and experimental values in the very low radial and axial positions due to neutralizer position effect. The high experimental values of temperature at radial distances greater than 70 mm for z=10 mm can be due to a reduction of thermal electrical conductivity caused by electron-ion collisions.

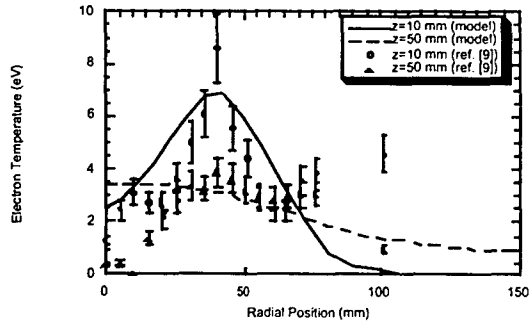

Fig. 3 - Measured [9] and computed electron temperature as a function of radial position for different axial position.

Acknowledgements

This paper was partially founded by the ASI under contract ARS IC-142-00-0. The authors thank Gianpiero Colonna (IMIP, CNR) for providing the set of e/Xe cross-sections.

References

[1] V. V. Zhurin et al, *Plasma Source Sci. Technol.* **8** (1999) R1-R20.

[2] D. Y. Oh et al, *J. Propulsion and Power* **15** (1999) 345-357.

[3] I. D. Boyd, D. B. VanGilder, M. Keidar, *J. Spacecr. Rockets* **37** (2000) 129-136.

[4] F. Taccogna, S. Longo, M. Capitelli, *AIAA paper* **2000-2345** (2000).

[5] F. Taccogna, S. Longo, M. Capitelli, J. *Spacecr. Rockets* **39 (3)** (2002) 409-419.

[6] G. Colonna, L. D. Pietanza, M. Capitelli, *AIAA Paper* **2000-2349** (2000).

[7] R. Samanta Roy, *Ph. D. thesis, MIT* (1995).

[8] K. Nanbu, Y. Kitatani, *J. Phys. D: Appl. Phys.* **28** (1995) 324-330.

[9] S. Kim, J. E. Foster, A. D. Gallimore, *AIAA paper* **96-2972** (1996).